Geomechanics, Anisotropy and LMR

Marco Perez *, Apache Canada Ltd, Calgary, AB, Canada
marco.perez@apachecorp.com
Bill Goodway, Apache Canada Ltd, Calgary, AB, Canada
bill.goodway@apachecorp.com
David Close, Apache Canada Ltd, Calgary, AB, Canada
david.close@apachecorp.com

Summary

Estimating subsurface stresses through seismic data can provide invaluable information for drilling and hydraulic stimulation efforts. Methods for estimating such stresses, however, are inherently non-unique. Understanding how the seismic response varies as a function of subsurface stresses, mapped into Lambda-Mu-Rho (LMR) space and subsequently compared to observed data, is a useful interpretation tool. This methodology allows different subsurface stress regimes to be considered equally until such a point that available data corroborates or contradicts a given model. With data from the Horn River Basin, BC, it is shown that relating patterns in LMR cross-plots to engineering parameters, which are not easily explained by variations in lithology or elastic moduli, can be, at least partly, understood by considering the effects of stress.

Method

There are many different formulations for estimating horizontal subsurface stresses. A common starting point is the passive basin assumption where the horizontal stress is a function of the overburden (σ_{zz}) and Poisson's ratio (ν),

$$\sigma_{xx} - p = \frac{\nu}{1-\nu}\left(\sigma_{zz} - p\right) \quad 1.$$

where p is the pore pressure. Stress measurements that deviate from this equation require adjustments to the passive basin assumption. These adjustments invoke various physical models, such as anisotropic media (Iverson, 1995), a fault stress equilibrium model (Wu et al., 1998), or Hooke's Law (Sayers, 2010). The model explored herein is Hooke's law as it pertains to stress induced seismic anisotropy and the concept of rock strength.

The stress estimation method we employ herein is adapted from the passive basin equation, also known as the minimum closure stress equation, which has the general form of

$$\sigma_{xx} - p = \frac{\lambda}{\lambda + 2u}\left(\sigma_{zz} - p\right) + \psi \quad 2.$$

This was recast by Goodway et al. (2010) in terms of lambda-mu-rho (LMR) for seismic applications and can be used to estimate the minimum horizontal stress. Figure 1 shows equation 2 on a crossplot of minimum and maximum effective stress. The slope of the lines in Figure 2 are given by $\lambda/(\lambda+2\mu)$ and the intercept is ψ.

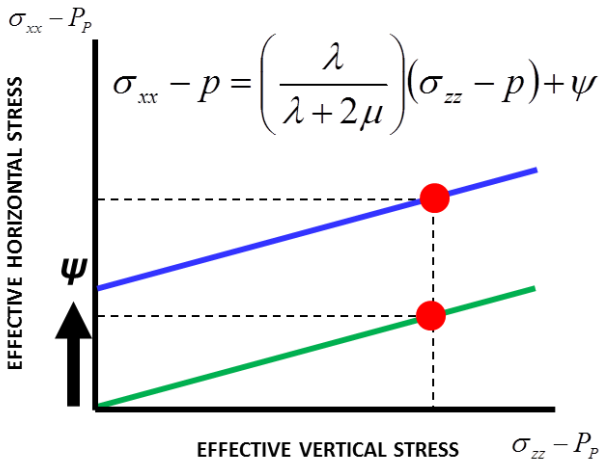

Figure 1. Plot of horizontal stress relationship.

The input parameters required to solve for the minimum horizontal stress are:

1. The ratio of $\lambda/(\lambda+2\mu)$, called the closure stress scalar (Goodway et al. 2006, 2010), which can be estimated from inverted seismic data. It can also be expressed as v / (1- v) where v is Poisson's ratio.
2. The effective overburden stress can be estimated by integrating a density log and knowledge of the local pressure gradient or pore pressure analysis using seismic velocities (Bowers, 1995; Sayers et al., 2002)

Estimating the second term, ψ, can be much more difficult. The model considered here describes ψ as a tectonic effect, where lateral strains are permitted and ψ, derived from Hooke's Law, is defined by Sayers (2010) as

$$\psi = \frac{E}{1-\upsilon^2}\left(\varepsilon_h + \upsilon\varepsilon_H\right) \quad 3.$$

and recast in terms of λ and μ by Goodway et al. (2006, 2010) as

$$\psi = \frac{\lambda}{\lambda+2\mu} 2\mu\left(\frac{\varepsilon_{yy}^2 - \varepsilon_{xx}^2}{\varepsilon_{yy}}\right) \quad 4.$$

and labelled the tectonic elastic strain energy term. Goodway et al. (2010) also demonstrates how the tectonic strain energy term relates to the anisotropic parameter γ and how it could manifest in seismic data. Given a definition of γ as

$$\gamma = \frac{Vs_1^2 - Vs_2^2}{2Vs_2^2} \quad 5.$$

where Vs_1 and Vs_2 are the fast and slow shear velocity respectively, Goodway et al. (2010) introduces the term γ' defined as

$$\gamma' = \frac{Vs_2^2}{Vs_1^2}\left(\frac{Vs_1^2 - Vs_2^2}{2Vs_2^2}\right) = \left(\frac{Vs_1^2 - Vs_2^2}{2Vs_1^2}\right) \approx \frac{1}{2}\frac{\varepsilon_{yy}^2 - \varepsilon_{xx}^2}{\varepsilon_{yy}^2} \quad 6.$$

so that

$$2\mu\varepsilon_{yy}\left(\frac{\varepsilon_{yy}^2 - \varepsilon_{xx}^2}{\varepsilon_{yy}^2}\right) \approx Vs_1\gamma' \quad 7.$$

Assuming that γ is a measurement of γ', estimating γ can be related to subsurface stress induced anisotropy.

To estimate ψ from seismic reflection data, amplitude variation with azimuth (AVAZ) is used to determine the magnitude of the anisotropy, represented by Thomsen's parameters of ε, δ, and γ (Thomsen, 1986). Ruger (1998) derived a linearized expression for AVAZ approximated to two terms by two of the three Thomsen parameters, δ and γ. More specifically, the anisotropic gradient term has the form of

$$B_{ani} = \frac{1}{2}\left(\Delta\delta^{(v)} - 8\left(\frac{Vs}{Vp}\right)^2 \gamma \right) \qquad 8.$$

Perez (2010) illustrated the effect of anisotropic AVAZ data on an isotropic inversion and how anisotropic data would manifest itself in LMR crossplot space. The important term in determining the amount of anisotropy is the discriminant, defined as

$$dis = \frac{1}{4}\left(\frac{Vp}{Vs}\right)^2 \Delta\delta^{(V)} + 2\Delta\gamma \qquad 9.$$

Figure 2 illustrates the direction which one would expect to see anisotropic effects for two distinct combinations of anisotropic parameters.

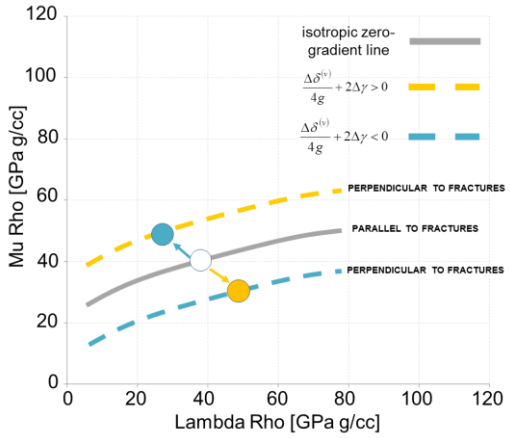

Figure 2: Manifestation of anisotropic data in LMR space where g = $(Vs/Vp)^2$.

From a seismic perspective ψ (Equation 4) can be written as,

$$\psi = \frac{\lambda}{\lambda + 2\mu} 2\sqrt{\frac{\mu}{\rho}\gamma} \qquad 10.$$

Once stresses are estimated, they can be used in rock failure applications. A popular model for rock failure, and a theoretical basis for hydro-fracture stimulation, is the Mohr-Coulomb failure criterion. Expressed in terms of maximum and minimum principle stresses,

$$\sigma_3 = \frac{1-\sin\phi}{1+\sin\phi}\sigma_1 - 2C_o\frac{\cos\phi}{1+\sin\phi} \qquad 11.$$

where C_o is the *cohesion* of the rock and ϕ is the angle of internal friction, as defined by the Mohr-Coulomb criteria (Jaeger et al., 2007).) In the Mohr-Coulomb plane, the failure criterion slope is the coefficient of internal friction, η, an imaginary surface internal to a rock before it fails. The angle that the line makes is the angle of internal friction, defined as $\phi = \tan^{-1}\eta$. Cohesion, (C_o) can be thought of as the amount of shear stress required for an intact rock to fail without any applied normal stress (unconfined). Figure 3 illustrates the Mohr's circle and failure criteria in both the $\sigma_1 - \sigma_3$ plane and the shear – normal stress plane.

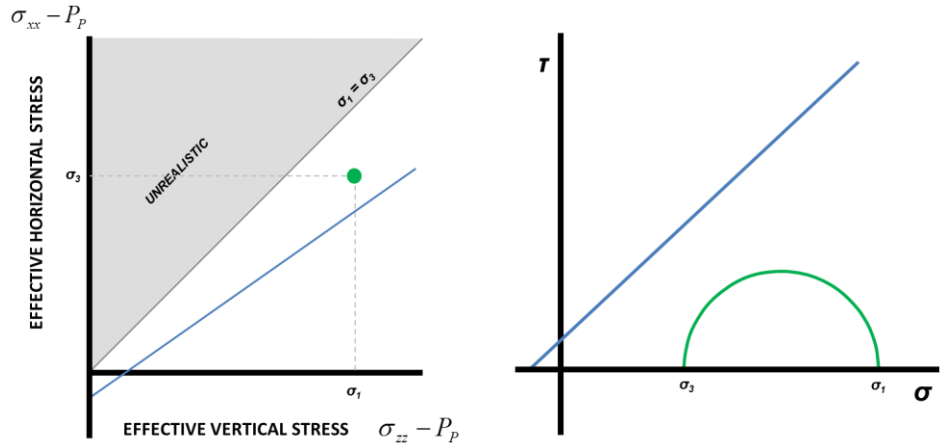

Figure 3. Mohr Coulomb failure criterion in the σ1 – σ3 plane (left) and the shear – normal stress plane (right). The green dot represents the Mohr-Coulomb circle in $\sigma_1 - \sigma_3$ plane

To map out seismic expressions of stress, the angle of internal friction, ϕ, can be expressed in LMR terms by making the following equivalency

$$\frac{\lambda}{\lambda + 2\mu} = \frac{1 - \sin\phi}{1 + \sin\phi} \qquad 10.$$

which results in

$$\phi = \sin^{-1}\left(\frac{\mu}{\lambda + \mu}\right) \qquad 11.$$

The term $(\cos\phi)/(1+\sin\phi)$ also can be expressed in terms of λ and μ as

$$\left(\frac{\cos\phi}{1+\sin\phi}\right) = \sqrt{\frac{\lambda}{\lambda + 2\mu}} \qquad 12.$$

Figure 4a shows an LMR crossplot with lines of constant Young's modulus (asymptotic to lines of constant μ at high λ values), and where ϕ follows Poisson's Ratio (Figure 4b).

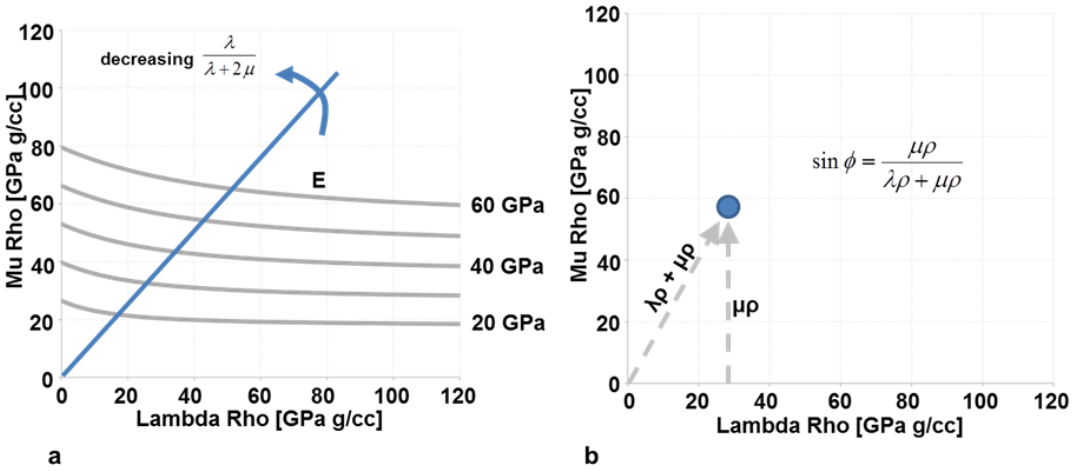

Figure 4: a) Lines of constant Young's modulus in LMR space illustrates that for large λρ, E becomes proportional to μρ. b) Angle of internal friction in LMR space plots in the same manner as Poisson's ratio, increasing in clockwise direction from the μρ axis.

Interpreting the LMR crossplot space with this model, one expects lower horizontal stresses with high μρ and low λρ, but higher horizontal stresses with higher λρ.

Combining both concepts, the closure stress equation and the Mohr-Coloumb failure criterion, on to a singular $\sigma_1 - \sigma_3$ plane, the relationship between the two models can be seen and it can be used to describe hydraulic stimulation engineering parameters (Figure 5).

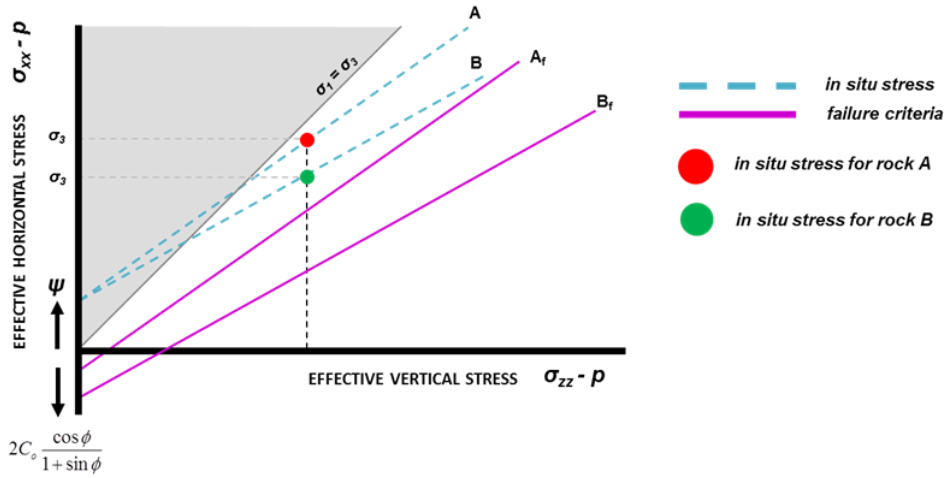

Figure 5. Crossplot of in-situ stress estimate (Equation 2) and the Mohr-Coulomb failure criterion for two different rock types.

Examples

Using data from the Horn River Basin, BC, it is clear that even within a single basin different models explain patterns observed in LMR cross-plot space. To understand this from an LMR perspective, seismically derived LMR data is plotted and color coded by Instantaneous Shut-In Pressure (ISIP), which is used as a proxy for minimum horizontal stress. Two examples are shown, one demonstrating the applicability of ψ manifested as seismic anisotropy in γ and the other as a rock strength term.

The first example is meant to demonstrate ψ as a tectonic strain energy term. Figure 6 shows seismically derived crossplots of two well pads, one of which crosses a major structure.

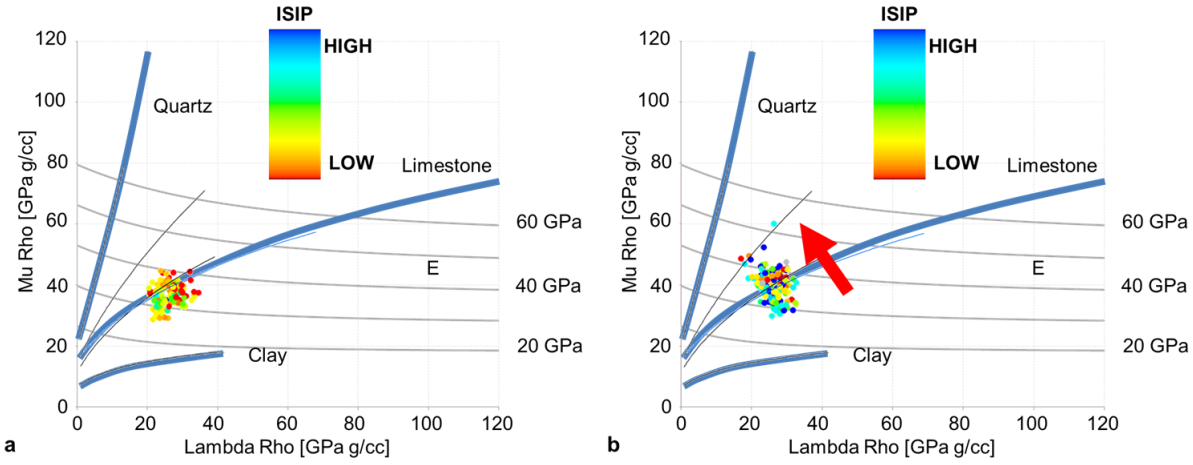

Figure 6. LMR crossplot of seismically derived rock properties color coded by ISIP. Plot A shows a lower ISIP values and has no visible anisotropic effect (unstressed) and does not intersect a mapped fault. Plot B has a higher ISIP values and shows an anisotropic inversion expression, interpreted as stress and intersects seismically detectable fault.

Data included in Figure 6a clusters tightly in LMR space, whereas data from the pad that intersects the major structure (Figure 6b) trends from a similar origin towards higher $\mu\rho$ and lower $\lambda\rho$. The discrepancy between LMR values is interpreted to be an inversion expression of stress induced HTI

anisotropy. The stress induced data is also characterized by higher ISIP values, which could be accounted for by greater values of ψ.

The second example demonstrates how ψ acts as a rock strength term. Figure 7 shows a crossplot of seismically derived LMR values color coded by ISIP values. In general as inverted values trend towards higher $\mu\rho$, the ISIP values (a proxy for closure stress) also increase. In addition, trending in a clockwise direction from the $\mu\rho$ axis there is also an increase in ISIP for similar values of $\mu\rho$, particularly at the 50 GPa g/cc $\mu\rho$ value, a consequence of $\lambda/(\lambda+2\mu)$. In this case the subsurface stress does not manifest in AVAZ analysis.

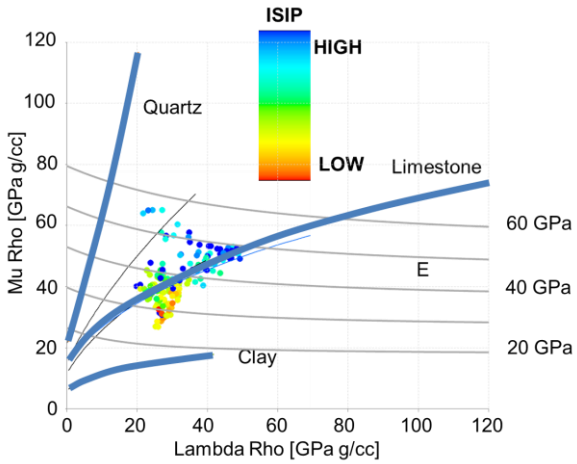

Figure 7. LMR crossplot of seismically derived seismic rock properties color coded by ISIP.

If one considers the Gurevich et al. (2011) stress induced anisotropic model, the induced HTI anisotropy is elliptical and Thomsen's parameters are a function of the ratio of the fractures normal and tangential compliances. The discriminant, defined in Perez (2010), then is a function of *Vp/Vs* ratio and the fracture compliance ratio, *B*. Which implies that the seismic expression of HTI can be reduced by variations in *B* (Figure 8).

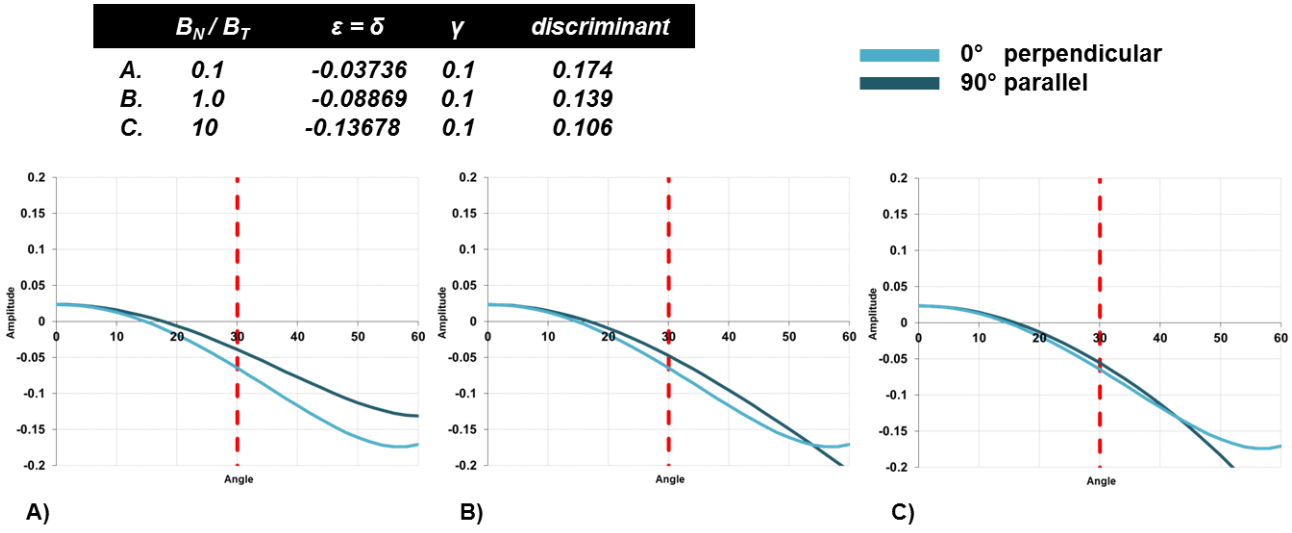

Figure 8. Varying *B* ratios accounting for varying amounts of anisotropic discriminant. Note that as *B* increases the discriminant, and thus ability to detect anisotropy using azimuthally varying amplitudes, is diminished.

Note that for large values of *B* the HTI expression is reduced. It is interpreted that this is the case for example 2 and as such the crossplot in Figure 7 is a function of $\lambda/(\lambda+2\mu)$ and μ.

Conclusions

Seismic attributes can be used to constrain predictions of ISIP. Knowledge obtained from seismic data can provide additional information regarding stress state and, therefore, assist in high-grading lower frack effort reservoir zones or by pointing out potentially difficult stages. The non-uniqueness of the stress estimation problem is somewhat circumvented by employing multiple models to explain the pressure data. Using multiple models, generating seismic interpretation templates and integrating engineering data can yield better performing completion programs.

Acknowledgements

Author would like to thank the contributions of Greg Purdue.

References

Sayers, C., 2010, Geophysics under stress: geomechanical applications for seismic and borehole acoustic waves, SEG DISC.

Goodway, B., Perez, M., Varsek, J. and Abaco, C., 2010, Seismic petrophysics and isotropic-anisotropic AVO methods for unconventional gas exploration, The Leading Edge, 29 , no. 12, 1500-1508,

Jaeger, J. C., Cook, N. G. W. and Zimmerman, R., Fundamentals of Rock Mechanics, 4th Edition. Wiley-Blackwell, 2007.

Bowers, G. L., 1995, Pore Pressure Estimation From Velocity Data: Accounting for Overpressure Mechanisms Besides Undercompaction, SPE, 27488.

Thomsen, L., 1986, Weak elastic anisotropy, Geophysics, 51, no 10, 1954-1966.

Rüger, A., 1997, P-wave reflection coefficients for transversely isotropic models with vertical and horizontal axis of symmetry, Geophysics, 62 , no. 3, 713-722.

Gurevich, B., Pervukhina, M., and Makarynska, D., 2011, An analytic model for the stress-induced anisotropy of dry rocks. Geophysics, Vol. 76, No 3, WA125-WA133.

Wu, Addis and Last 1998, Stress Estimation in Faulted Regions: The Effect of Residual Friction, SPE/ISRM 47210

Tsvankin, I., 1997, Anisotropic parameters and P-wave velocity for orthorhombic media, Geophysics, 62 , no. 4, 1292-1309.

Perez, Marco, 2010, Beyond Isotropy – Part 2: A Prestack Perspective, Recorder 35 - No 8, 36-41.

Iverson, W. P., 1995, Closure Stress Calculations in Anisotropic Formations, SPE, 29598.

Goodway, B., Chen, T. and Downton, J., 1997, Improved AVO fluid detection and lithology discrimination using Lamé petrophysical parameters; “λρ”,“μρ”,&“λ/μ fluid stack”, from P and S inversions, SEG Expanded Abstracts, 16, no 1, 183-186.